

High Shear Strain Rate Rheometry of Polymer Melts

A. L. Kelly, T. Gough, B. R. Whiteside, P. D. Coates

IRC in Polymer Engineering, School of Engineering, Design and Technology, University of Bradford, West Yorkshire, Bradford BD7 1DP, United Kingdom

Received 4 November 2008; accepted 19 March 2009

DOI 10.1002/app.30552

Published online 15 June 2009 in Wiley InterScience (www.interscience.wiley.com).

ABSTRACT: The rheology of a range of polymer melts has been measured at strain rates above those attained during conventional rheometry using an instrumented injection molding machine. Deviations from shear thinning behavior were observed at high rates, and previously unreported shear thickening behavior occurred for some of the polymers examined. Measured pressure and volumetric throughputs were used to calculate shear and extensional viscosity at wall shear strain rates up to 10^7 s^{-1} . Parallel plate rheometry and twin bore capillary rheometry were used to provide comparative rheological data at low and medium shear strain rates, respectively. Commercial grades of polyethylene, polypropylene, polystyrene, and PMMA were studied. Measured shear viscosity

was found to follow Newtonian behavior at low rates and shear thinning power law behavior at intermediate strain rates. At shear strain rates approaching or above 10^6 s^{-1} , shear viscosity reached a rate-independent plateau, and in some cases shear thickened with further increase in strain rate. A relationship between the measured high strain rate rheological behavior and molecular structure was noted, with polymers containing larger side groups reaching the rate-independent plateau at lower strain rates than those with simpler structures. © 2009 Wiley Periodicals, Inc. *J Appl Polym Sci* 114: 864–873, 2009

Key words: rheology; viscosity; injection molding; micromolding; capillary rheometry

INTRODUCTION

Rheological characterization of polymer melts is a widely used technique for quality control, process design, simulation, and troubleshooting applications.^{1,2} Commonly used techniques include those using rotational, capillary, or slit flows which approximate viscometric flow conditions at a series of set strain rates and temperatures. Such characterizations are generally carried out in a laboratory environment to obtain accurate measurements at well-controlled conditions. In-process rheological characterization can be used for some applications such as for process-sensitive polymers, or for feedback control purposes, but limitations in the strain rate range attainable and disturbance to the process are potential disadvantages to such methods.³

The recent drive toward manufacture of molded components on a microscale and thin sections has led to the development of high-speed injection molding processes such as micromolding, small scale, and thin-walled injection molding. Such processes use high injection speeds through small gates to improve cavity filling on rapid timescales to prevent melt freezing. Subsequently, the extreme flow rates, thermal transients, and cycling of pressures

encountered are beyond the range of melt flow conditions which have previously been studied. The focus here is melt rheology at extremely high strain rates. Attainable shear strain rates in rotational rheometry are limited to around 10^3 s^{-1} and around 10^5 s^{-1} in capillary rheometry. Wall shear strain rates in micromolding and thin-walled molding can exceed 10^7 s^{-1} . Therefore, there is a need to measure, understand, and predict flow behavior of polymer melts at such high shear strain rates to feed simulation models and assist process design and material development.

Rheological behavior of polymer melts measured at high strain rates (above 10^5 s^{-1}) has not been widely reported. Groves et al.⁴ found a good agreement in shear viscosity between results from off-line rheological characterizations and in-line measurements made using an injection molding machine up to shear strain rates of 10^5 s^{-1} . Haddout et al.^{5,6} measured the rheology of several polymer melts during the injection molding process using a cylindrical instrumented nozzle with variable diameter. Pressure drop was measured at three locations along the length the nozzle allowing shear viscosity to be calculated. Additionally, by assuming linear pressure drop along the nozzle, exit pressure could be extrapolated, allowing the first normal stress difference to be determined. Polypropylene and high-density polyethylene were found to follow pseudo-plastic shear thinning behavior up to shear strain rates of around 10^6 s^{-1} , above which they reached a

Correspondence to: A. L. Kelly (A.L.Kelly@Bradford.ac.uk).

“quasi-Newtonian plateau.” Such behavior was attributed to a shift in glass transition with increasing pressure effectively canceling out any shear thinning. A similar behavior was observed for glass fiber reinforced polypropylene using the same system.⁶

Takahashi et al.⁷ reported rheological measurements made using a hydraulically powered capillary rheometer up to wall shear strain rates of 10^7 s^{-1} for a range of polymer melts. Observed flow curves exhibited a second Newtonian plateau at shear strain rates above 10^6 s^{-1} and a second shear thinning region above these rates. This second shear thinning region was attributed to chain scission of the polymer backbone and a generalized flow curve was proposed to explain the behavior of various polymer melts. Specialist rotational rheometers for high strain rates have also been reported, using small gap sizes between parallel plates to strain rates above 10^6 s^{-1} for lubricant systems.⁸

The aim of the work reported here was to investigate the high strain rate rheological behavior of a range of polymers, using a high accuracy state of the art electric injection molding machine designed for high-speed injection of thin-walled products. For the first time, apparent extensional rheology has been examined in addition to shear behavior at extreme processing rates. Experimental results are presented for a range of polymers, and the validity of making measurements at such high pressures and short time scales is discussed.

RHEOLOGICAL CHARACTERIZATION

Capillary rheometry is a pressure-driven technique in which pressure drop is measured across a capillary die at a known flow rate to calculate viscosity. By repeating these measurements at a range of volumetric throughputs, the strain rate-dependent viscosity, or “flow curve” can be determined. Typically, measurements are made using two capillary dies, one with a length to diameter ($L : D$) ratio above 10 : 1 to generate a shear dominated flow, and an orifice die with the same diameter but $L : D$ ratio < 1 , to generate an “entry” flow which is expected to be dominated by extensional flow.

During flow of polymer through the die apparent shear rate and shear stress at the wall of a cylindrical die can be derived from the Poiseuille law⁹:

$$\dot{\gamma}_{\text{app}} = \frac{4Q}{\pi R^3} \quad (1)$$

$$\tau_{W,\text{app}} = \frac{R\Delta P}{2L} \quad (2)$$

where $\dot{\gamma}_{\text{app}}$ and $\tau_{W,\text{app}}$ denote apparent wall shear rate (s^{-1}) and shear stress (Pa), respectively for flow

of fluid through a capillary having radius R (m) and length L (m), at volumetric flow rate Q (m^3/s) across pressure drop ΔP (Pa). Apparent shear viscosity is the ratio of apparent shear stress to shear rate:

$$\eta_{\text{app}} = \frac{\tau_{W,\text{app}}}{\dot{\gamma}_{\text{app}}} \quad (3)$$

Newtonian fluids in laminar flow exhibit a parabolic velocity profile, whilst for polymer melts the flow profile tends to be plug-like. The relationship between $\dot{\gamma}_{\text{app}}$ and $\dot{\gamma}_{\text{true}}$ as shown in eq. (4) has been derived considering a balance of forces for flow through the capillary.

$$\dot{\gamma}_{\text{true}} = \left(\frac{3n+1}{4n} \right) \times \dot{\gamma}_{\text{app}} \quad (4)$$

To accurately measure the wall shear stress, the pressure drop across the die should be corrected for the energy required to converge the melt into the entrance of the capillary by measuring the entrance pressure drop. The true, or Bagley corrected wall shear stress (τ) is calculated as:

$$\tau_w = \frac{(\Delta P_L - \Delta P_o) \times R}{2L} \quad (5)$$

where ΔP_o and ΔP_L denote pressure drop at the die entrance and across the die length, respectively. ΔP_o is an indicator of flow convergence and in turn an extensional property of the melt. Extensional viscosity is a measure of a material's resistance to tensile or stretching flow, and a number of direct and indirect measurements have been proposed.^{10–13} Cogswell¹⁰ treated the analysis of convergent flow by separating the convergent flow into shear and extensional components. This has been modified to treat free convergence (entry semi-angle 90°). It is a simple and widely used extensional viscosity analysis.

$$\eta_E = \frac{9}{32} \frac{(n+1)^2}{\eta} \left(\frac{P_o}{\dot{\gamma}} \right)^2 \quad (6)$$

$$\sigma_E = \frac{3}{8} (n+1) P_o \quad (7)$$

$$\dot{\gamma} = \frac{\sigma_E}{\eta_E} \quad (8)$$

where η_E , σ_E , and $\dot{\epsilon}$ are extensional viscosity (Pa s), extensional stress (Pa), and extensional rate (s^{-1}), respectively. The above derivations are based on the assumptions that flow is isothermal, incompressible, axisymmetrical and that the velocity at the die wall is zero. Errors caused by heat generation and pressure effects on viscosity^{14,15} are often assumed to be

mutually canceling.¹⁶ The validity of these assumptions, which hold reasonably well for capillary rheometry at conventional polymer processing strain rates, is questionable at the extreme strain rates examined in this study, and will be discussed in relation to the experimental results later. The temperature dependence of shear viscosity is an important parameter in-process design and simulation, and a number of models have been used. The simplest of these is an exponential dependence where:

$$f(T) = e^{-b(T-T_r)} \quad (9)$$

T and T_r are the temperature and a reference temperature, respectively, and b is the temperature sensitivity ($^{\circ}\text{C}^{-1}$) of viscosity. This model is accurate over a small temperature range, whereas the Arrhenius¹⁷ and Williams, Landel and Ferry (WLF)¹⁸ models are also used to describe temperature sensitivity over a wider temperature range.

EXPERIMENTAL

Low strain rate measurements ($10^{-1} - 10^2 \text{ s}^{-1}$) were made on an Anton-Paar MCR301 rheometer using a 25 mm diameter parallel plate geometry with a gap size of 1 mm and a strain of 5%. This value is within the linear viscoelastic regime for all melts tested. Shear and extensional rheology at intermediate strain rates ($10-10^5 \text{ s}^{-1}$) was studied using a twin bore RH10 capillary rheometer (Malvern Instruments, UK). Dual pistons of diameter 15 mm were used to drive melt flow through capillary dies at speeds up to 20 mm/s with a maximum crosshead force of 100 kN. Three pairs of capillary dies with entry angle of 180° were used to attain a wide range of shear strain rates. These diameter of these dies were 2 mm, 1 mm, and 0.25 mm. In each case, one barrel of the rheometer was fitted with a capillary die with an $L : D$ ratio of 16 and the other bore was fitted with an orifice die. Capillary dies were made from tungsten carbide-cobalt alloy in order to maintain tight geometrical integrity. The polymer was subjected to precompression pressures of 1.0 and 0.5 MPa for the long and orifice dies respectively, and subjected to a total preheating time of 540 s. Set crosshead speeds were chosen to provide the maximum attainable strain rate range for each capillary die set, within the limits of the melt volume and pressure transducer range. Pressure transducers were selected to provide the appropriate range for the pressures generated during each test, from 3.5 to 206.8 MPa.

For high strain rate rheometry, a Fanuc Roboshot 1000-i injection molding machine was used, with screw diameter 22 mm and a maximum barrel pressure rating of 260 MPa. The machine was operated

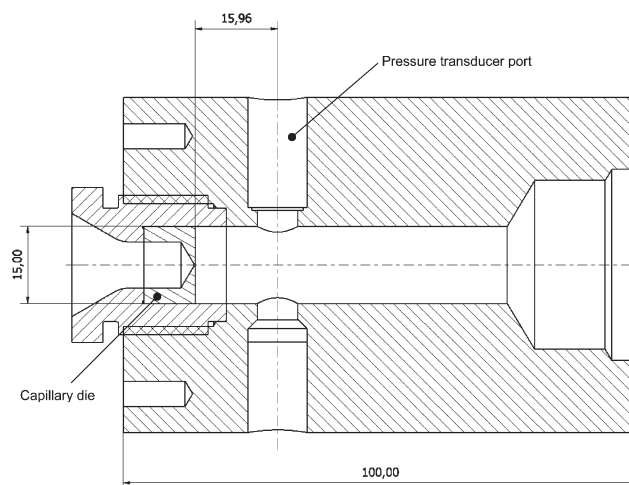


Figure 1 Instrumented nozzle adaptor showing location of pressure transducers and capillary die (dimensions in mm).

in air-shot mode using a capillary die in place of the nozzle. Melt pressure was measured at the entrance to the capillary die at a frequency of 100 Hz using two types of pressure transducer – a Dynisco PT435 and a Kistler 4015A, as shown schematically in Figure 1. Injection screw position and speed were also monitored at the same frequency. Each polymer was injected at a range of speeds from 1 mm/s to 150 mm/s first through a capillary die of length 4.0 mm and diameter 0.5 mm, then these tests were repeated with an orifice die of the same diameter. Polymer was plasticized in the screw of the molding machine at a screw rotation speed of 1.67 revolutions per second with at back pressure of 4 MPa. Injection was initiated following a dwell time of 60 s. Process data were collected using a LabView SC2345 data acquisition unit triggered by a 24 V signal from the injection molding machine at the start of injection.

Nine polymers were examined as listed in Table I. Linear and long chained branched polyethylenes were characterized to examine the effect of branching, polypropylene homopolymers, polystyrene and a linear and branched PMMA were also measured. All characterizations were carried out at a set temperature of 200°C , with the exception of the PMMAs which were tested at 230°C .

RESULTS AND DISCUSSION

Accuracy of set injection speed

A precise volumetric throughput is required to use an injection molding machine as a capillary rheometer. Figure 2 shows measured injection velocities at three set values representative of the range used throughout these characterizations. The three set velocities of 25, 75, and 125 mm/s correspond to

TABLE I
Details of the Polymers Studied

Polymer type	Trade name	Grade	Manufacturer	M_w	M_w/M_n	Test temperature (°C)
PP (homo)	–	HP561R	Moplen	192,000	3.5	200
PP (homo)	–	100-GA12	Ineos	283,000	7.5	200
HDPE	Rigidex	HD5050EA	Ineos	88,500	5.6	200
HDPE	Rigidex	HD6007EA	Ineos	93,300	5.4	200
LDPE	–	LD150E	Dow	221,000	17.5	200
LDPE	Lupolen	1840H	Basell	190,000	14.0	200
PS	Glaskar	158K	BASF	274,000	2.5	200
PMMA (linear)	–	MS983	Lucite Int.	110,600	2.1	230
PMMA (branched)	–	P1EXP195	Lucite Int.	304,200	2.5	230

uncorrected wall shear strain rates through a 0.5 mm diameter capillary die of 0.77, 2.32, and $3.87 \times 10^6 \text{ s}^{-1}$, respectively. At each set velocity, the screw exhibited an initial acceleration, followed by a slight overshoot, and stabilized at the set velocity within 200 ms. Assuming negligible back flow over the check ring, the volumetric throughput for each set velocity can be accurately determined.

Figures 3 and 4 show measured capillary die pressure drops through the 0.5 mm diameter long and orifice dies, respectively at the three injection velocities displayed in Figure 2. In each case, measured pressures were observed to increase after initial injection and stabilized within the time taken for the shot volume to be discharged. The time taken for pressure to reach equilibrium was found to decrease with increasing volumetric throughput. Only in the case of the highest injection speed through the long die had the measured pressure not conclusively reached an equilibrium value, but it appeared to be closely approaching this case. This potential inaccuracy will be discussed in relation to the observed rheological characterizations in more detail below.

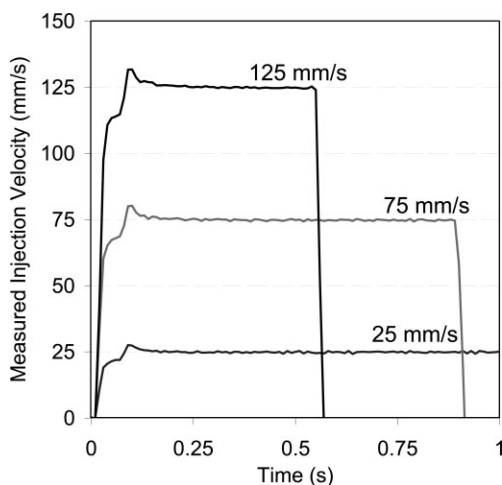


Figure 2 Measured injection velocities at set values 25, 75, and 125 mm/s; LDPE at 200°C.

Shear viscosity

Measured shear viscosities of two grades of polypropylene across a shear strain rate range of 10^{-1} to 10^7 s^{-1} are shown in Figure 5. A good agreement was observed between the three techniques considering the differences in flow regimes and geometries used. Shear viscosity of both polypropylenes decreased from around 1000 Pa s at low strain rates to less than 1 Pa s at highest rates, and three distinct regions of strain dependent behavior were observed. The melts exhibited Newtonian behavior at low strain rates (below 1 s^{-1}) and pseudo-plastic shear-thinning behavior at strain rates up to around 10^5 s^{-1} . Above these rates the behavior deviated from shear thinning, reaching a quasi-Newtonian plateau at approximately 10^6 s^{-1} . Measurements made at the highest rates for one of the grades (HP561) appeared to show a shear thickening viscosity behavior. These results are broadly in line with the findings of Haddout and Villoutreix⁵ for a different grade of the same polymer, and have implications for the upper achievable limits of high-speed injection processes.

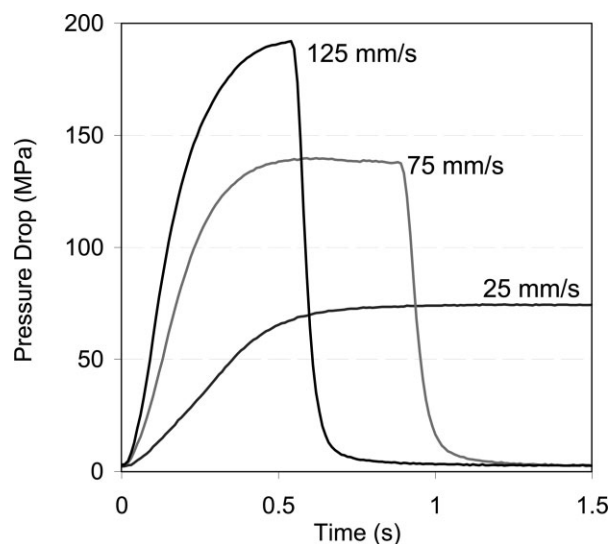


Figure 3 Measured long die pressure drop for at set injection speeds of 25, 75, and 125 mm/s; LDPE at 200°C.

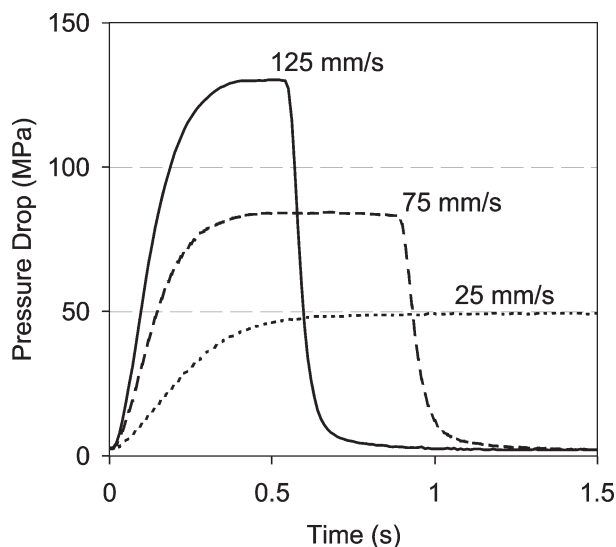


Figure 4 Measured orifice die pressure drop at set injection speeds of 25, 75, and 125 mm/s; LDPE at 200°C.

Molecular weight appeared to have a significant effect on the behavior of the two grades at low and high strain rates, whereas at intermediate levels the two measured viscosities were overlaid. This suggests that molecular size or structure may influence the observed high strain plateau. From the observed rheological behavior, it is obvious that a single shear thinning index “ n ” cannot be determined from the capillary rheometry data across the medium and high shear strain rate regions. For simplicity and to avoid artificial discontinuities in the flow curves a single value of “ n ,” taken in the pseudo-plastic

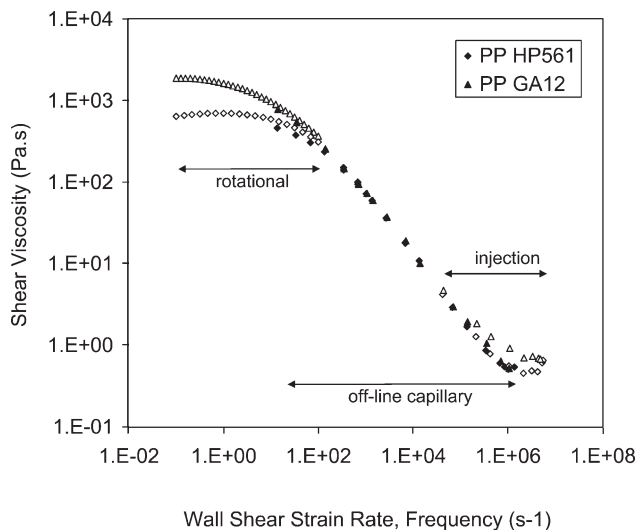


Figure 5 Shear viscosity of polypropylene measured at 200°C; open symbols denote parallel plate rheometry below 10^2 s^{-1} and injection molding rheometry above 10^4 s^{-1} , filled symbols denote off-line capillary rheometry.

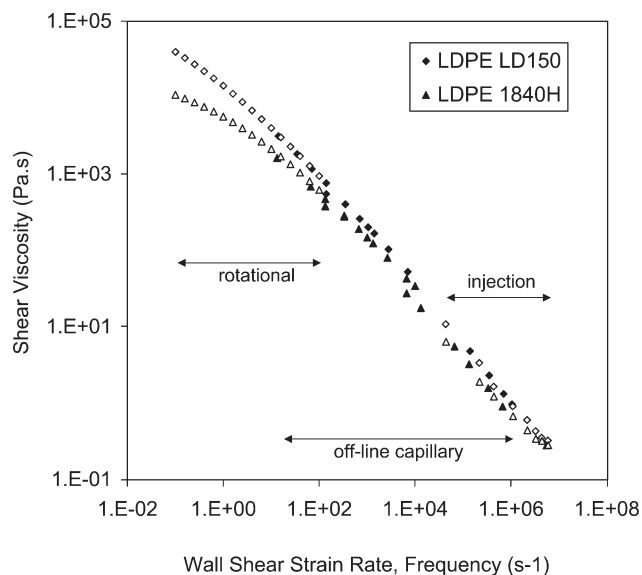


Figure 6 Shear viscosity of low-density polyethylene measured at 200°C; open symbols denote parallel plate rheometry below 10^2 s^{-1} and injection molding rheometry above 10^4 s^{-1} , filled symbols denote off-line capillary rheometry.

region, has been used to apply the Rabinowitsch correction to wall shear strain rates in this study.

Shear viscosity data for low-density and high-density polyethylenes are displayed in Figures 6 and 7, respectively. For these polymers, nonlinearities in shear viscosity at high rates were less apparent. Shear viscosity appeared to deviate from pseudo-plastic behavior only at the highest rates examined, suggesting that a simple model such as the power

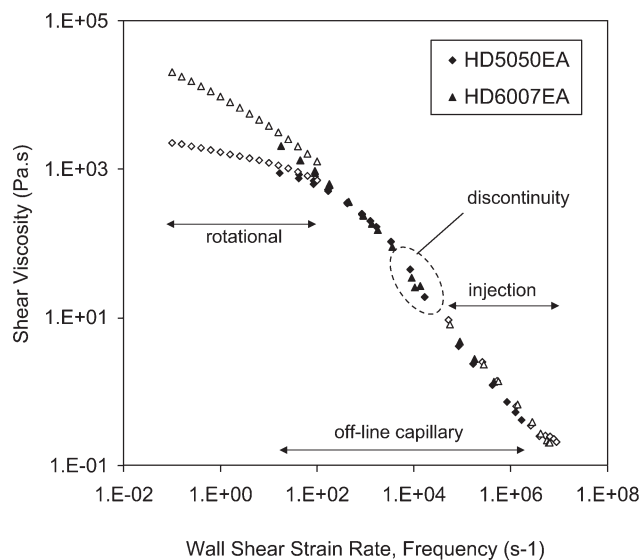


Figure 7 Shear viscosity of high-density polyethylene measured at 200°C; open symbols denote parallel plate rheometry below 10^2 s^{-1} and injection molding rheometry above 10^4 s^{-1} , filled symbols denote off-line capillary rheometry.

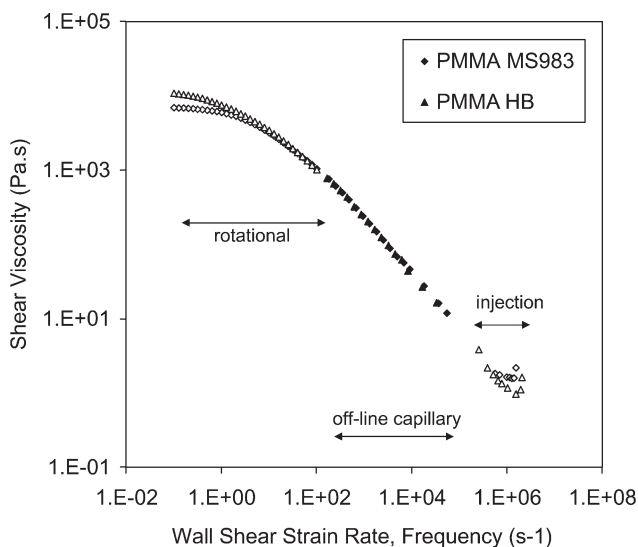


Figure 8 Shear viscosity of polymethylmethacrylate at 230°C; open symbols denote parallel plate rheometry below 10^2 s^{-1} and injection molding rheometry above 10^4 s^{-1} , filled symbols denote off-line capillary rheometry.

law could be used to describe shear viscosity over a wide strain rate range, up to $\sim 10^6 \text{ s}^{-1}$. Long chain branching appeared to have a relatively minor effect on the observed high strain rate behavior, the only noticeable difference between LDPE and HDPE being a discontinuity in the shear viscosity of HDPEs at strain rates around 10^4 s^{-1} due to melt flow instabilities.¹⁹

Shear viscosities of two grades of PMMA are displayed in Figure 8, one being linear (MS983) and one having medium levels of branching (HB). As with the previous materials, Newtonian behavior

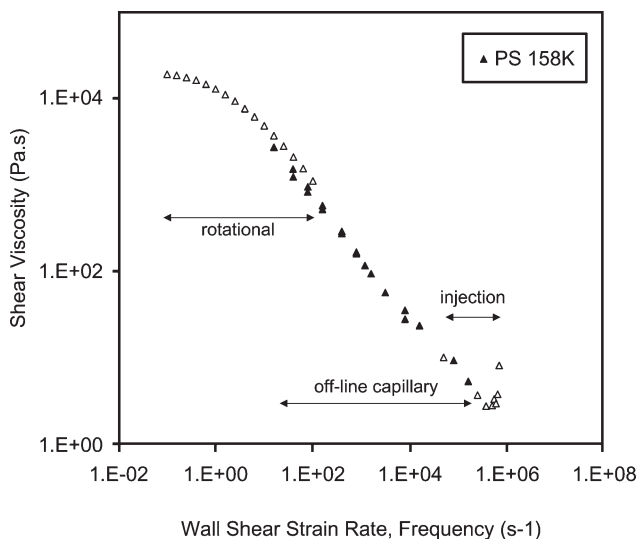


Figure 9 Shear viscosity of polystyrene at 200°C; open symbols denote parallel plate rheometry below 10^2 s^{-1} and injection molding rheometry above 10^4 s^{-1} , filled symbols denote off-line capillary rheometry.

was observed at low strain rates and pseudo-plastic behavior at intermediate strain rates. In common with measurements made with PP, significant differences between the shear viscosity of the two materials was observed in the Newtonian region, whereas at intermediate strain rates the shear viscosities were almost identical. At strain rates above $5 \times 10^5 \text{ s}^{-1}$, a strain independent plateau and inflection toward shear thickening was observed for both polymers. This inflection was more pronounced than the corresponding behavior in PP, and occurred at a lower onset strain rate. Branching appeared to have the effect of increasing viscosity at low strain rates and decreasing viscosity at high strain rates. Shear viscosity of polystyrene is shown in Figure 9. As with PMMA, a clear inflection in the measured shear viscosity occurred at strain rates above $5 \times 10^5 \text{ s}^{-1}$.

The observation of a high strain rate plateau and in some cases an inflection indicative of dilatant shear flow behavior is an important one which has widespread implications for high-speed injection processes. The rapid shift from shear thinning to thickening for PS and PMMA suggests that in practice, melt under injection exhibits a rapidly increasing resistance to flow above a critical injection velocity. The reasons for this behavior are as yet unclear, although several factors may contribute. First, pressures of up to 260 MPa were generated in time scales of less than 1 s. Temperature rises due to adiabatic compression within this period will also be significant, as will temperature rises due to shear heating generated in the capillary die. Crystallization forced by the high pressures has been suggested to explain the deviation from shear thinning behavior at high strain rates⁶ and at low temperatures,²⁰ although it would appear unlikely that such a mechanism would affect predominately amorphous PS more readily than semicrystalline PE. Perhaps, a more significant contribution is played by the effect of pressure on viscosity. Sedlacek et al.¹⁴ and Couch and Binding¹⁵ measured the effect of pressure on shear viscosity for a number of polymers up to pressures of 70 MPa. Pressure sensitivity of different polymers was found to be directly linked to molecular structure; those polymers with larger side chain groups had a higher sensitivity to pressure. Figure 10 shows the molecular structure repeat unit of the

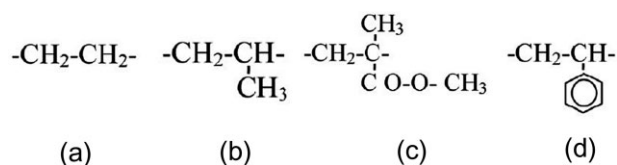


Figure 10 Molecular structure of the four polymer types characterized. (a) Polyethylene, (b) polypropylene, (c) polymethylmethacrylate, and (d) polystyrene.

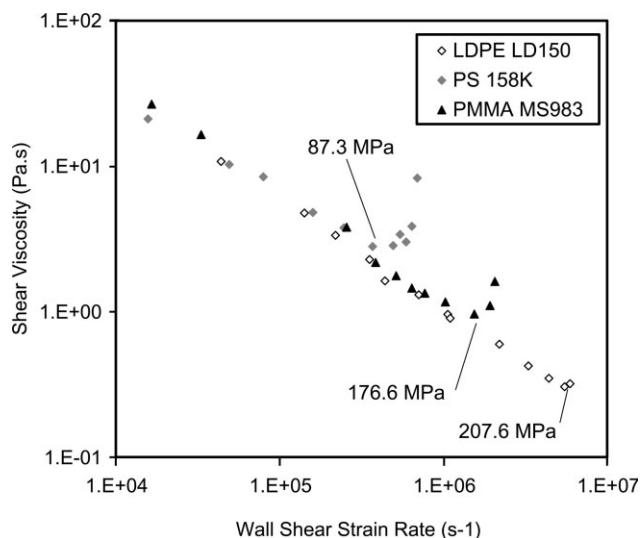


Figure 11 Comparison of shear viscosity of different polymers at high shear strain rates.

four different types of polymer characterized during the present study. According to the structure, the polymers may be ordered in terms of the complexity as PE > PP > PMMA > PS. Figure 11 compares measured shear viscosities for three of the polymer types examined, which exhibited a similar shear viscosities in the shear thinning region. The onset strain rate at which deviation from shear thinning behavior occurred is ordered as PS < PMMA < (PP) < PE (results for polypropylene have been omitted from the Figure to improve clarity). This correlation suggests that pressure effect, dependent upon molecular structure, may play a significant role in the shear viscosity plateau and shear thickening. Coefficients of sensitivity of shear viscosity to pressure and temperature as reported by Sedlacek¹⁴ are shown in Table II. A clear correlation between the pressure and temperature sensitivity and complexity of molecular structure can be seen. Figure 11 shows the measured long die pressure drop at which each of these three polymers reached an inflection in shear viscosity. These pressures increased from PS > PMMA > PE, corresponding to decreasing values of pressure and temperature sensitivity of viscosity.

The second shear thinning region reported by Takahashi et al.⁷ above the second Newtonian plateau was not observed during the course of the current work. The reasons for this discrepancy are unclear. If the reported phenomena is real, a possible explanation is that the current study did not reach high enough strain rates, the main limitation being the pressure limit of the injection molding machine barrel (260 MPa). PS melt was injected at velocities up to 10 times greater than those at which the limiting pressure was first reached in an attempt to transcend the shear thickening region, but in each

case the limiting pressure of the injection molding machine was reached. It is not clear whether the same level of accuracy of injection velocity achieved in the molding machine used here was attained in the hydraulic system reported earlier.⁷ The response time of sensors and data acquisition equipment may also have been slower than current systems, which in turn may have affected accuracy of results at the highest injection velocities. Another significant difference between the two measurement systems was the static melting used in the earlier reported study, compared to the screw-driven melting method used in the injection molding machine here and more widely used in commercial polymer processing.

Extensional viscosity

Molecular chains approaching a maximum backbone stretch at the entrance to the die may be another contributory factor to the high strain rate behavior observed here. To explore this further, we examine the extensional component of flow as measured using the orifice die. Figure 12 shows extensional viscosity, calculated using Cogswell's free convergence model¹⁰ for polystyrene from twin bore and injection molding capillary rheometry. Here, extensional viscosity followed a tension thinning behavior. A corresponding plot for LDPE, as displayed in Figure 13, shows clear extensional hardening was observed for both grades studied. This was also in contrast to the observed shear viscosity behavior and explains why, for polyethylenes exhibiting shear thinning behavior at rates above 10^6 s^{-1} , maximum shear strain rates were limited to 10^7 s^{-1} before the upper pressure limit of the machine barrel was reached. The results suggest that there are different mechanisms which restrict the upper limiting shear strain rate at which a melt can be injected; dilatant shear flow and dilatant extensional flow behavior. It should be noted that the entrance pressure drop values used in the calculated of extensional viscosity

TABLE II
Sensitivity of Shear Viscosity to Pressure and Temperature Reported by Sedlacek¹⁴

Polymer type	Pressure sensitivity (GPa^{-1}) ^a	Temperature sensitivity ($10^{-3} \text{ }^\circ\text{C}^{-1}$) ^b
HDPE	9.99	13.85
LDPE	18.27	26.23
PP	27.25	34.66
PMMA	51.41	82.70
PS	61.55	78.41

^a Measured at 190°C except for PMMA measured at 230°C .

^b Measured at pressure 70 MPa.

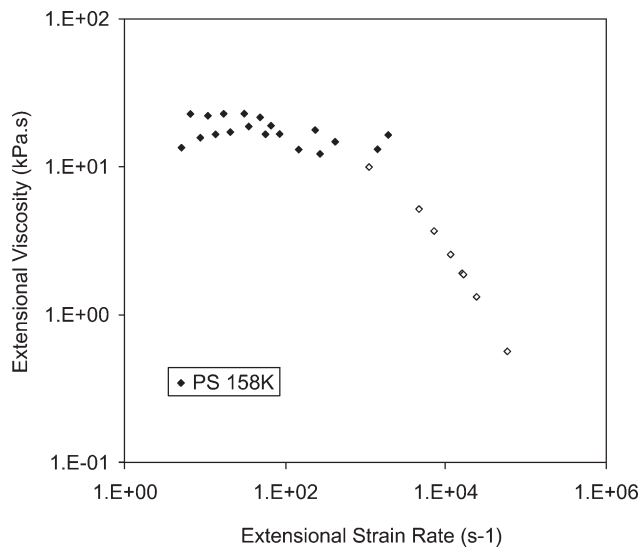


Figure 12 Extensional viscosity of polystyrene at 200°C; open symbols denote injection molding rheometry, filled symbols denote off-line capillary rheometry.

also contain a less significant proportion of pressure drop due to first normal stress difference. Figure 14 shows entrance pressure drop across the orifice die as a percentage of the corresponding long die pressure drop, i.e. $(\Delta P_0/\Delta P_1 \times 100)$ for the two extremes of polymers examined (HDPE and PS). For the majority of polymers studied, entrance pressure increased dramatically compared to long die pressures, to the extent where at the highest strain rates examined, entrance pressure drop contributed to over 80% of the long die pressure drop. In the cases of PS and PMMA, this value reached a maximum at

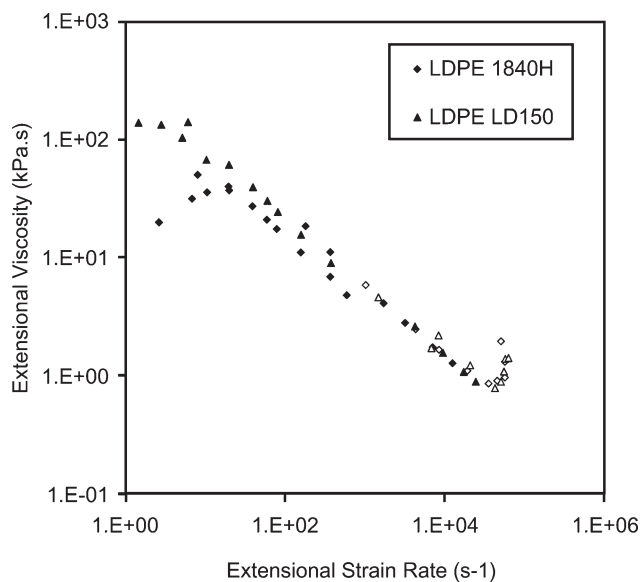


Figure 13 Extensional viscosity of LDPE at 200°C; open symbols denote injection molding rheometry, filled symbols denote off-line capillary rheometry.

shear rates corresponding to the inflection in shear viscosity and then dropped, as shown for PS.

Validity and assumptions

The validity of precision rheological measurements made using proprietary polymer processing machinery over short time frames should be examined more closely. From Figures 1–3, we have established that the set injection velocity was achieved and that measured pressures appeared to stabilize within the time frame of the shot volume being discharged, suggesting a relatively stable flow regime. Only at the highest injection velocities was there a suggestion that measured pressures through the long die may be under predicted if the values had not stabilized before shot completion. Leakage flow of polymer melt over the check ring during injection is another potential source of error and quantitative measurements of leakage flows do not appear in the open literature. However, empirical studies within our laboratories and marketing literature published by manufacturers of modern all-electric precision molding machines suggest that leakage flows are minimal and as such may be considered negligible for the purposes of this study. Reynolds number at the highest injection velocities and lowest shear viscosities was calculated to be up to 1420 and therefore within the limits of laminar flow. Overall, the sources of potential error from the characterization method are minimal, and the effects of any errors in leakage flow or under-estimation of stabilized pressure would lead to an apparent reduction in

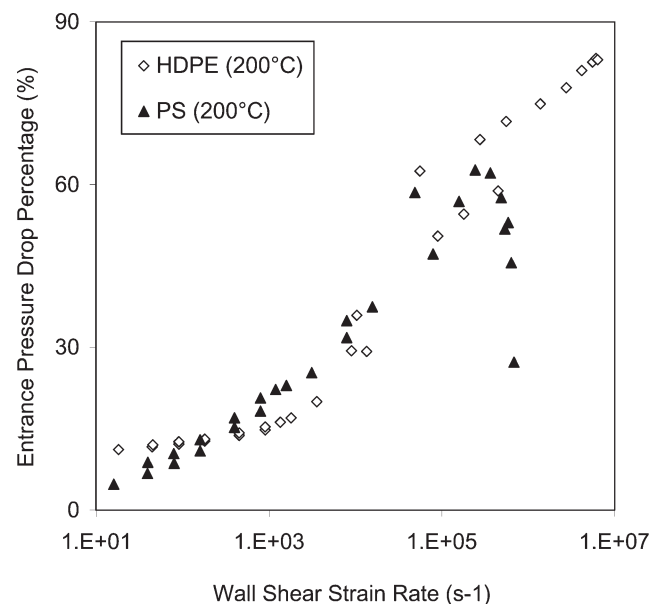


Figure 14 Entrance pressure drop as a percentage of long die pressure drop measured during twin bore and injection molding capillary rheometry.

TABLE III
Predicted Shift in Viscosity Due to Temperature $f(T)$ and Pressure $f(P)$ for Three Polymers Flowing Through a Long Capillary Die at a Pressure of 100 MPa

Polymer	Density (kg/m ³)	C_p (J/kg K)	α (10 ⁻³ °C ⁻¹)	β (GPa ⁻¹)	ΔT compression (°C)	$f(T)$	$f(P)$
HDPE	732	3300	14	10	41.4	-1.8	+2.9
PP	784	2720	25	22	46.9	-3.2	+9.0
PS	970	1975	60	43	52.2	-22.9	+73.7

viscosity and therefore would not explain the observed high strain rate behavior.

A previous common assumption in capillary rheometry that pressure and temperature effects on viscosity are comparable in magnitude but opposite in sign and therefore mutually canceling should also be questioned for the high strain rates and pressures attained in the current work. As already discussed, pressure effects on viscosity have been studied only up to pressures of 70 MPa and it is therefore difficult to predict the effects at pressures up to 260 MPa generated in this study. The influence of pressure on viscosity can be described by the Barus equation:

$$\eta = \eta_0 \cdot e^{\beta P} \quad (10)$$

where η_0 represents viscosity at ambient pressure, P is the gauge pressure, and β is the pressure coefficient. The influence of temperature on viscosity can be described by a similar exponential function:

$$\eta = \eta_r \times e^{-\alpha(T-T_r)} \quad (11)$$

where η_r represents the viscosity at reference temperature T_r , T is the measured temperature and α is the temperature coefficient of viscosity. The theoretical temperature rise due to work done during adiabatic compression can be calculated using the first law of thermodynamics:

$$\Delta T = \frac{\Delta P}{\rho \times C_p} \quad (12)$$

where ΔT represents temperature rise caused by a change in pressure of ΔP , ρ is the melt density, and C_p is the specific heat capacity. Predicted temperature rises due to adiabatic compression for HDPE, PP, and PS flowing through a 4 × 0.5 mm capillary die are shown in Table III, at a melt pressure of 100 MPa. Estimated viscosity shift due to pressure and temperature dependence using eqs. (10) and (11) are also shown, using values of α and β obtained from literature.^{14,15} From this table, it is clear that PS is more significantly affected by changes in pressure and temperature than HDPE and PP. For all three polymers, the magnitude of shift in viscosity was higher for pressure effects than for temperature, at a pressure of 100 MPa. Therefore, it appears likely that the pressure effect on viscosity is related to the

observed rheological behavior at high pressures. Further analysis of the effects of pressure and temperature on viscosity are necessary at higher pressures than previously reported. It should also be noted that the reported values of sensitivity to temperature and pressure, α and β , vary significantly across different studies, and as such the values used will have a large influence on any predicted effects on viscosity.

These simple theoretical calculations of the effects of pressure and temperature do not take into account viscous shearing or dissipation of heat, although more detailed analysis of pressure and viscous heating effects have been reported.²¹ Direct measurement of melt temperature at such high pressures and short time frames is challenging²² and raises issues such as the effect of high rate convergent flows with large extensional strains causing chain orientation in the flow direction, with consequent anisotropy of heat conduction influencing heat transfer. However, such measurements are necessary to further understand the observed rheological behavior and are the subject of ongoing investigation within our laboratories. Although the fundamental understanding of the mechanisms causing the rheological phenomena observed in this study require further research, it is clear that the results have direct implications for high rate injection processes.

CONCLUSIONS

Polymer melt rheology was measured from wall shear strain rates of 10⁻¹ to 10⁷ s⁻¹ for a range of polymers. Good agreement was observed between shear viscosities measured using three techniques used to span a wide strain rate range. Measured shear viscosity exhibited a deviation from pseudo-plastic shear thinning behavior at high strain rates, initially following a Newtonian type plateau and then in some cases demonstrating shear thickening behavior. The onset strain rate at which shear viscosity deviated from shear thinning behavior appeared to be linked to molecular structure; polymers with larger side groups such as polystyrene reaching a Newtonian plateau at lower rates than those of polypropylene and polyethylene. The behavior of effective extensional viscosity, calculated from measured

entrance pressure drop, contrasted that of shear viscosity at high strain rates. For polymers with simple molecular structure, an inflection in extensional viscosity was measured whereas for more complex molecular shape, extension thinning behavior occurred at high strain rates. The relative importance of entrance pressure drop, as a function of the total pressure drop across the capillary die increased dramatically as strain rate increased, for all polymers examined. The observed high strain rate behavior is thought to be influenced by pressure effects on viscosity at the extreme pressure gradients encountered. The measured results are significant for the design and simulation of high-speed injection processes such as micromolding and thin-walled injection molding.

References

1. Collyer, A. A. *Techniques in Rheological Measurement*; Chapman and Hall: Cambridge, 1993.
2. Whorlow, R. W. *Rheological Techniques*, 2nd ed.; E. Horwood: New York, 1992.
3. Dealy, J. M.; Broadhead, T. O. *Polym Eng Sci* 1993, 33, 1513.
4. Groves, D. J.; Martyn, M. T.; Coates, P. D. *Plast Rubber Compos Process Appl* 1997, 26, 13.
5. Haddout, A.; Villoutreix, G. *Int Polym Proc* 2000, 15, 291.
6. Benhadou, M.; Haddout, A.; Villoutreix, G. *J Reinf Plast Compos* 2007, 26, 1357.
7. Takahashi, H.; Matsuoka, T.; Kurauchi, T. *J Appl Polym Sci* 1985, 30, 4669.
8. Mriziq, K. S.; Dai, H. J.; Dadmun, M. D.; Jellison, G. E.; Cochran, H. D. *Rev Sci Instrum* 2004, 75, 2171.
9. Rauwendaal, C. *Polymer Extrusion*, 2nd ed.; Hanser Publishing: Munich, 1990.
10. Cogswell, F. N. *Trans Soc Rheol* 1972, 16, 383.
11. Gibson, A. G. *Converging Dies*; Chapter 3 of *Rheological Measurements*; Collyer, A. A.; Clegg, D. W., Eds. Elsevier Applied Science: New York, 1988.
12. Binding, D. M. *J Non-Newtonian Fluid Mech* 1988, 27, 173.
13. Sentmanat, M. L. *Rheol Acta* 2004, 43, 657.
14. Sedlacek, T.; Zatloukal, M.; Filip, P.; Boldizar, A.; Saha, P. *Polym Eng Sci* 2004, 44, 1328.
15. Couch, M. A.; Binding, D. M. *Polymer* 2000, 41, 6323.
16. Cogswell, F. N. *Polymer Melt Rheology: A Guide for Industrial Practice*; Godwin: London, 1981.
17. Mendelson, R. A. *Polym Eng Sci* 1968, 8, 235.
18. Williams, L.; Landel, R. F.; Ferry, J. D. *J Am Chem Soc* 1955, 77, 3701.
19. Agassant, J. F.; Arda, D. R.; Comeaud, C.; Merten, A.; Mundstedt, H.; Mackley, M. R.; Rober, L.; Vergnes, B. *Int Polym Proc* 2006, 11, 239.
20. Aho, J.; Syrjala, S. *Polym Test* 2007, 27, 35.
21. Cho, B. *Polym Eng Sci* 1985, 25, 1139.
22. Bur, A. J.; Roth, S. C. *Polym Eng Sci* 2004, 44, 898.